Available online at www.sciencedirect.com
ScienceDirect
Cement & Concrete Composites 30 (2008) 622–638
Cement & Concrete Composites
www.elsevier.com/locate/cemconcomp

A study of reinforced concrete corner columns after fire

Wen-Chen Jau *, Kuo-Li Huang

Department of Civil Engineering, National Chiao-Tung University, 1001 Ta Hsueh Road, 300 Hsinchu, Taiwan

Received 20 November 2006; received in revised form 21 September 2007; accepted 25 September 2007
Available online 7 November 2007

Abstract

This study investigated the behavior of corner columns under axial loading, biaxial bending and asymmetric fire loading. It is found that, under a longitudinal stress ratio of $0.1f'_c$, the residual strength ratios of the columns after fire loading show: (a) the 2 and 4 h fire loadings result in residual strength ratios of 67% and 57%, respectively; a 10% reduction on residual strength results as the duration changes from 2 to 4 h; (b) reductions in reinforcing steel ratio cause lower residual strength ratios; and (c) increasing the thickness of concrete cover causes lower residual strength ratios. It was also found that the temperature distribution across the cross-section is not affected by concrete cover thickness and steel ratio. The residual strengths can be used for future evaluation, repair and strengthening.

Keywords: Mechanical properties; High temperature; Residual strength; Residual strength ratio; Corner column; Reinforced concrete

1. Introduction

In recent years, many researchers, such as Lie [1–4]; Lin [5]; Ng [6,7]; Purkiss [8]; Lin [9–11]; Terro [12]; Kodur [13–19]; Dotreppe [20,21]; Zha [22]; Tan [23–25]; Faris [26]; Chung [27]; Persson [28]; Bratina [29]; and Benmarce [30,31] studied the fire safety behavior of concrete columns. These studies included experimental and analytical evaluations for columns made of normal strength concrete and high performance (or high strength) concrete. Most of these studies focused on the axial loading and four-sided fire loading, except for the study of Tan [25] who performed an analytical study for columns under non-symmetrical fire loading, although no experimental work was done to validate the results.

The behavior of reinforced concrete (RC) columns under high temperature is mainly affected by the strength of the concrete by the changes of material property and explosive spalling. Normal strength concrete (NSC), high strength concrete (HSC), high performance concrete (HPC), or self-compacting concrete (SCC) are commonly used in the RC columns. NSC has been defined as having compression strength below 42 MPa, while concrete with compressive strength higher than 42 MPa has been defined as HSC [32]. HPC may have high strength, high durability, and/or high modulus of elasticity [33]. SCC is an innovative concrete that does not require vibration for placing and compaction. It is able to flow under its own weight, completely filling formwork and achieving full compaction, even in the presence of congested reinforcement. The hardened concrete is dense, homogeneous and has at least the same engineering properties and durability as traditional vibrated concrete [34]. However, high temperatures affect the strength of the concrete by explosive spalling and so affect the integrity of the concrete structure. High strength concrete has a relative higher strength loss when exposed to the same heating condition than normal strength concrete, because high strength concrete is prone to explosive spalling.

Early research on the fire performance of concrete columns includes that done at the Portland Cement Association (PCA). Not only were material property studies conducted but also full-scale experiments under fire. Lie [1–8] established a thermal conductivity model and

* Corresponding author. Tel.: +886 3 5715255; fax: +886 3 5734111.
E-mail address: jau@mail.nctu.edu.tw (W.-C. Jau).

0958-9465/$ - see front matter © 2007 Elsevier Ltd. All rights reserved.
doi:10.1016/j.cemconcomp.2007.09.009

Nomenclature

T	average temperature in the furnace (°C)
t	time after the start of fire (min)
f_c	concrete compressive strength of high temperatures at a give strain ε_c (MPa)
f_r	concrete residual compressive strength of high temperatures (MPa)
f'_c	concrete compressive strength at 28 days (MPa)
ε_c	concrete strain (mm/mm)
f_y	yield stress of steel (MPa)
E_s	elastic modulus of steel (N/mm^2)
ε_s	strain of steel (mm/mm)
ε_y	yield strain of steel (mm/mm)
Δ_{ax}, Δ_{bx}	displacements from LVDT
$\varepsilon_{ax}, \varepsilon_{bx}$	strains calculated from Δ_{ax}, Δ_{bx} along X-axis at a and b
$\varepsilon_{fx}, \varepsilon_{ux}$	predicted strains at two edge along X-axis
φ_x	curvature of X-axis
P_n	approximate value of nominal load in biaxial with eccentricities e_x and e_y (kN)
P_{ny0}	nominal load when only eccentricity e_x is present ($e_y = 0$) (kN)
P_{nx0}	nominal load when only eccentricity e_y is present ($e_x = 0$) (kN)
P_0	nominal load for concentrically loaded column (kN)
k	thermal conductivity (W m^{-1} °C^{-1})
ρ	density (kg m^{-3})
c	specific (J kg^{-1} °C^{-1})

experimentally studied the effects of axial loading, cross-sectional dimensions, moisture content and various types of aggregates on the residual strength of interior concrete columns. Their results showed that both concentrically loaded and eccentrically loaded interior columns, designed according to ACI 318, have a nominal fire endurance of 3 h.

In 1988, Lin [9–11] conducted a series of experiments to investigate the residual strength and stiffness of fire-damaged and subsequently repaired columns under four-sided fire and eccentric axial loads in Taiwan. The results showed that most of the repaired columns could develop their original or even higher strength and stiffness or than those of the original columns.

From 1990 to 2006, more concrete columns experiments have been done for high strength concrete (HSC), high performance concrete (HPC), self-compacting concrete (SCC) and fiber-reinforced polymer (FRP) repaired RC columns. Kodur [13–17] performed a series of experiments at the National Research Council of Canada (NRCC) on the fire resistance of interior columns made of HSC. Data from this study indicated that the type of aggregate, concrete strength, load intensity, and detailing and spacing of ties could affect the fire resistance and performance of HSC columns. Furthermore, the test results also showed that the better tie configuration (bending of ties at 135° and provision of cross ties) and closer tie spacing have significant benefits on the fire resistance of HSC columns. Kodur also found that the fire resistance of a NSC column is higher than a HSC column. The addition of polypropylene fibers and the use of carbonate aggregate improved the fire resistance.

Kodur [18,19] also performed a research study on FRP-confined reinforced concrete columns. FRP in structural engineering applications involves repair and rehabilitation of existing RC columns by bonding a circumferential FRP wrap to their exterior. The experiments consisted of fire endurance tests on five RC columns: one unstrengthened circular and one unstrengthened square RC column, two circular FRP-wrapped and insulated RC columns, and one square FRP-wrapped and insulated RC column. Data obtained from the experiments shows that the fire behavior of FRP-wrapped concrete columns incorporating appropriate fire protection systems is as good or better than that of unstrengthened RC columns. Comparing the fire resistance of the circular columns, it was found that unstrengthened RC columns had a resistance of 245 min, whereas FRP-strengthened RC columns had a fire resistance greater than 330 min. This result is significant in that it demonstrates that the FRP strengthened columns are capable of providing satisfactory fire resistance under their strengthened service loads. In terms of the performance of the square columns, unstrengthened RC columns had a fire resistance of 262 min, whereas FRP-strengthened RC column had a fire resistance of 256 min. Again, the satisfactory fire behavior of the strengthened column under increased service loads can be attributed to the thermal insulation provided by the fire protection system.

The fire resistance of SCC is similar to that of NSC [34]. In general a low permeability concrete may be more prone to spalling, but the severity of the spalling depends upon the type of aggregate used, concrete quality and moisture content. SCC can easily achieve the requirements for high strength, low permeability concrete. The use of polypropylene fibers (PPF) in concrete has been shown to be effective in improving its resistance to spalling. The mechanism is believed to be due to the fibers melting and being absorbed in the cement matrix. The fiber voids then provide expansion chambers for steam, thus reducing the risk of spalling. Polypropylene fibers have been successfully used with SCC. Persson [28] suggested that one way to limit the amount of explosive fire spalling in columns with SCC to the same level as in columns with NSC is to introduce PPF into the concrete mix; another way was to keep the combination

of cement/powder and water/cement sufficiently high, a method that has been proven to be very effective.

In addition, predictive methods were developed and then compared to experimental results. The procedure includes two parts. The first part is the heat-transfer problem, which is to solve the heat-balance equation by finite difference method or finite element method. The temperature distribution across the concrete section can be obtained. The second part is the calculation of mechanical properties of the concrete material and concrete structures problem based on the temperature distribution from part 1. The methods can predict the fire endurance, the temperature distribution across the section, the strength of the column under fire, and the residual strength after the fire. These methods include:

(a) FRCP (fire resistance computer program) [6]: It analyzes the influence of selected parameters on the response and behavior of square reinforced concrete columns axially loaded and subjected to fire. The program calculates the internal temperature distribution of the column resulting from the external fire temperature using the finite difference method.
(b) SAFE-RCC (structural analysis of fire exposed reinforced concrete columns) [8]: The computer program called SAFE-RCC takes into account the change in load carrying capacity and stiffness of a column during a fire, as well as the change in stiffness of the framing system at each end of the column. Following the presentation of the results of some proving tests, it presents the results from an exploratory series of runs which clearly indicate that the flexural stiffness of the restraint system plays a large part in determining the fire response.
(c) SAFIR [20]: SAFIR is a finite element model that was developed at the University of Liege, Belgium, for the simulation of the behavior of a building subjected to fire. This software calculates the evolution of the temperatures in a structure subject to fire and the evolution of the equilibrium conditions (stresses, strains, displacements, moments, etc.) of the heated structure until failure. This model solves the transient analysis of the temperature in the structure and the mechanical analysis of the structure during the fire.
(d) European standards [21,29]: Eurocode 2 (2002) assesses the duration of the fire resistance of reinforced concrete columns and provides a simple formula for the duration of fire resistance of a reinforced concrete column as a member of a non-sway structure subjected mainly to compression.
(e) Extended ACI code [23–25]: The idea behind the extended ACI 318 code method is to find the ultimate failure points on the P–M interaction curves corresponding to different temperatures.
(f) Numerical method (transformed into a square network) [1,9–11,15–17,35,36]: This numerical method combined with the normal RC theory can be used to calculate the performance of RC columns during or after a fire. Assuming that the temperatures distribution within an element is constant and the element is homogeneous, the element is stacked to calculate the residual strengths. A further examination of these numerical modeling studies shows that these methods can be used both during fire and after a fire, and some literatures refer to his method as the lumped system method [35,36]. The methods (a)–(e) are used during a fire. Although the numerical method is an approximate method, many studies have proven it to be a good approach and could conveniently justified by experiment results. The numerical method is usually combined with the finite difference method or a package program to obtain the distribution of temperature of the concrete cross-section.

In the above-mentioned studies, the concerned is mainly on the fire-endurance of the column, and is especially focused on the spalling phenomenon for HSC columns, and only a few studies considered the residual strength of the column [1,9–11]. The main purpose of the present paper is to study the residual strength of RC columns subjected to only a two-sided fire exposure, axial loading and biaxial bending and to verify the applicability of a numerical method and RC theory. There are no previous similar tests available in the literature. This study employs the numerical method to justify the experimental of results.

2. Background

Corner columns are usually under high biaxial eccentricity. Furthermore, during a fire, only the interior two faces of corner columns may be exposed to fire in contrast to interior columns of which all four faces are exposed. The material asymmetry of concrete after fire further complicated the behavior of corner columns. This study investigated the behavior of corner columns under axial loading, biaxial bending and asymmetric fire loading. Six RC corner columns were manufactured for this research under high temperatures.

2.1. Fire laboratory

All experiments were performed in the fire laboratory of the Architecture and Building Research Institute (ABRI) in Gui-Ren, Tainan, Taiwan. The fire curve followed the Chinese National Standards (CNS) 12514 [37], which is the same as the curve from International Organization for Standardization (ISO) 834 [38]. The temperature change is as in Eq. (1). After two hours the temperature reaches 1049 °C, and after 4 h the temperature reaches 1153 °C, as shown in Fig. 1.

$$T = 345\log_{10}(8t + 1) + 20 \quad (1)$$

where T is the average temperature in the furnace (°C) and t is the time after the start of fire (minute).

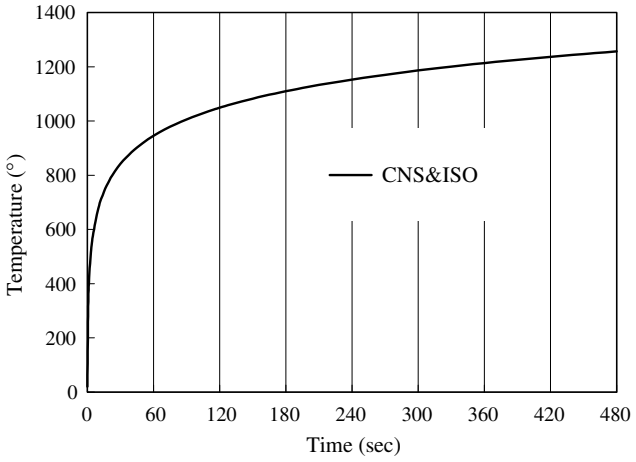

Fig. 1. Fire curve.

2.2. Material properties at elevated temperatures

The analysis of the concrete stress–strain curves of high temperatures (Fig. 2) follows Dr. Wen-Chen Jau's research result (2001) [39], as modified from Schneider and Haksever (1976) [40] and Lie (1986) [1]. The equations from Jau' test differ from Lie's are the residual strength ratio beyond 500 °C, especially beyond 700 °C, as shown in Fig. 3. The residual strength would be zero, according to Lie, around 700 °C, which is not found in this study. The present study compares the test result of 49 specimens [9] and compares them with those predicted by Jau and Lie. The results indicate that Jau's equation give a better prediction to the test result in Fig. 4. The averages of the predicted results strength/test results are 0.844 and 0.816, respectively with standard deviation of 0.207 and 0.224, based on Jau's and Lie's equations. The equations are as follows:

$$0\,^{\circ}\mathrm{C} \leqslant T \leqslant 500\,^{\circ}\mathrm{C}; \quad f_r = (1 - 0.001T) \times f'_c \tag{2}$$

$$500\,^{\circ}\mathrm{C} < T; \quad f_r = [1.6046 + (1.3T^2 - 2817T) \times 10^{-6}] \times f'_c \tag{3}$$

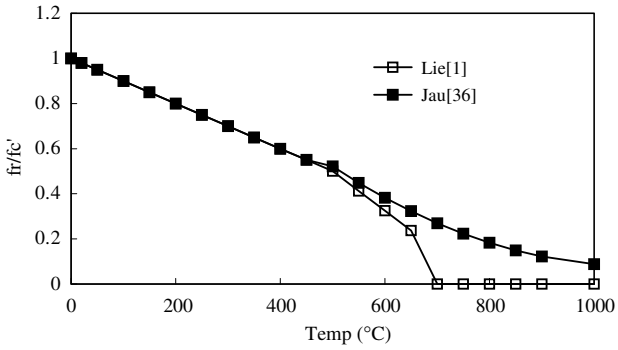

Fig. 3. Residue strength relation by Lie and Jau research.

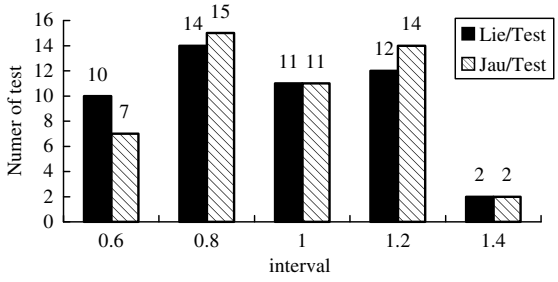

Fig. 4. Residue strength relation by Lie and Jau research.

$$\varepsilon_{max} = 0.0025 + (6T + 0.04T^2) \times 10^{-6} \tag{4}$$

$$\varepsilon_c \leqslant \varepsilon_{max}; \quad f_c = f_r \times \left[1 - \left(\frac{\varepsilon_{max} - \varepsilon_c}{\varepsilon_{max}}\right)^2\right] \tag{5}$$

$$\varepsilon_c > \varepsilon_{max}; \quad f_c = f_r \times \left[1 - \left(\frac{\varepsilon_c - \varepsilon_{max}}{3\varepsilon_{max}}\right)^2\right] \tag{6}$$

where T is the temperature (°C); f_c the concrete compressive strength of high temperatures at a give strain ε_c (MPa); f_r the concrete residual compressive strength of high temperatures (MPa); f'_c the concrete compressive strength at 28 days (MPa); ε_c the concrete strain (mm/

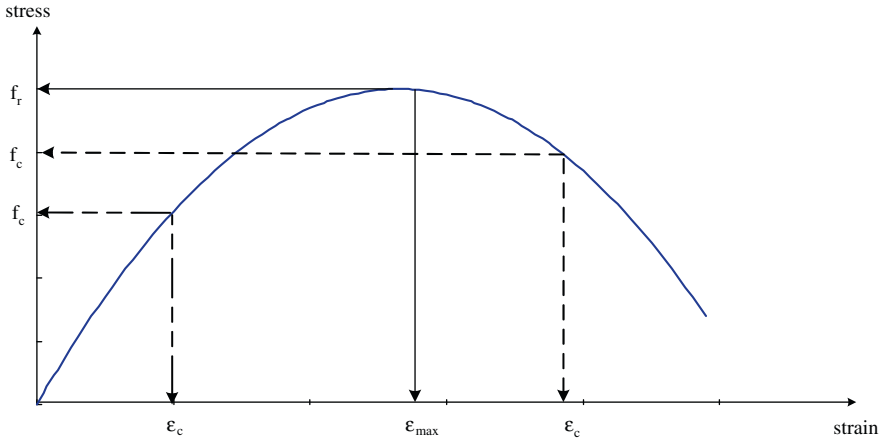

Fig. 2. The stress–strain relationship of concrete of high temperature.

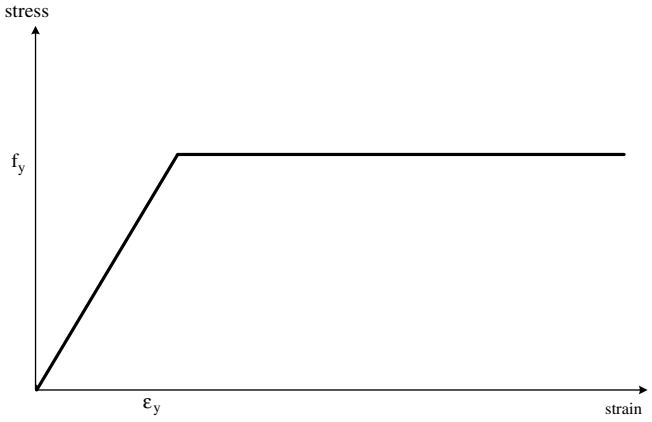

Fig. 5. The stress–strain relationship of steel of high temperature.

mm); and ε_{max} is the max. concrete strain at given temperature (mm/mm).

The steel behavior of high temperatures in the range of the experimental test (below 700 °C) shows a negligible change and existing stress–strain curves (Fig. 5) are used [1,9–11,41] and follow Eqs. (7) or (8).

$$f_s = E_s\varepsilon_s; \quad \varepsilon_s \leqslant \varepsilon_y \tag{7}$$

$$f_s = f_y; \quad \varepsilon_s > \varepsilon_y \tag{8}$$

where f_y is the yield stress of steel (MPa); f_s the stress of steel (MPa); E_s the elastic modulus of steel (N/mm^2); ε_s the strain of steel (mm/mm); and ε_y is the yield strain of steel (mm/mm).

3. Experiment studies

The three experimental steps include:

(1) Specimen manufacture: to fabricate steel cages, concrete casting, and curing.
(2) Fire test: specimens are put into a furnace in a group of four columns to simulate corner columns during a fire, as shown in Figs. 6 and 7.
(3) Strength tests: to determine the axial strength of the column under a given eccentricity for each column. The columns can be fire loaded or non-fire loaded.

3.1. Specimens

RC columns with dimensions of $300 \times 450 \times 2700$ mm were cast for this study. The design material strength were $f'_c = 27.6$MPa (the test strength was 33.7 MPa) and $f_y = 413.8$ MPa (the test strength was 475.87 MPa). Two rebar sizes, No. 8 (φ 25 mm) and No. 10 (φ 32 mm), were used as longitudinal reinforcement and No. 4 (φ 13 mm) steel was used for ties spaced at 100 mm (Fig. 8). The design follows the ACI 318 code [42]. Column size is commonly used for 3-storey buildings. The steel ratio was 2% and 3%; the cover was 50 mm (non precast, exposed to earth) and a cover of 70 mm for comparison.

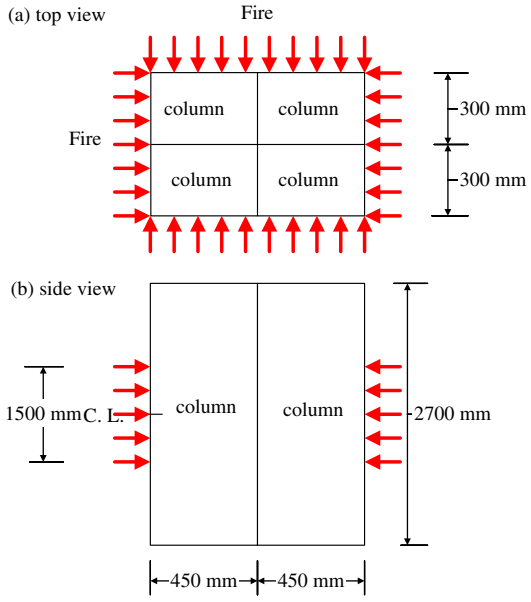

Fig. 6. A sketch map of column specimens under high temperature.

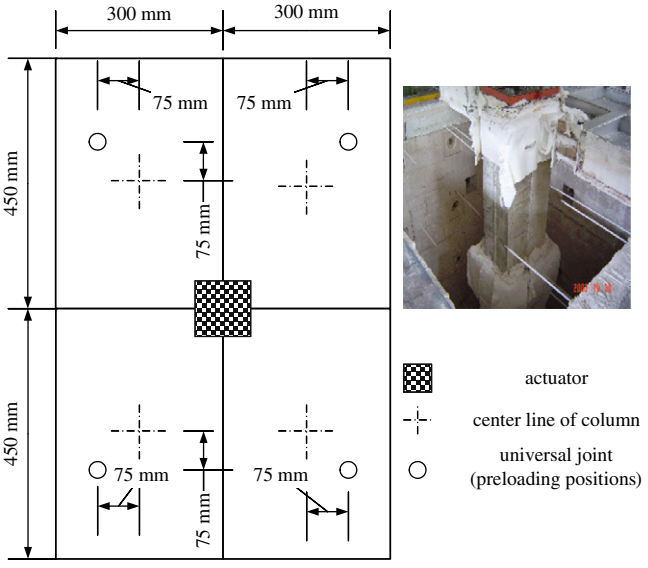

Fig. 7. Column arrangement and load application during fire test.

The mix design of concrete is listed in Table 1. The columns were tested at least 1.5 years after casting and were kept in air to reduce the moisture content within the concrete. To determine the temperature changes throughout the tests, K-type thermocouples were embedded in the middle height of the columns at different locations as shown in Fig. 9. Table 2 shows the location of thermocouples.

Spalling often occurs in HSC (over 42 MPa), because there are fewer pores in HSC. As a result, the steam vapor cannot escape easily from inside the concrete to the surface. On the other hand, NSC (below 42 MPa) is more porous than HSC and the vapor can escape to air easier. The concrete compressive strength is 27.6 MPa in this study and was air-dried for 1.5 years. Ties of 135° hook were used to avoid spalling of concrete.

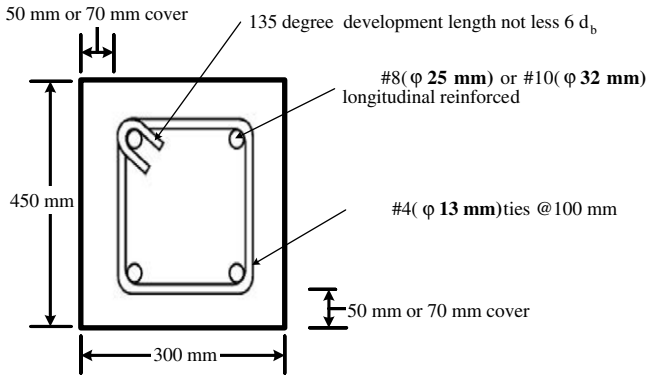

Fig. 8. Column cross-section.

Table 1
Mix proportions for the concrete

Property	Mix
Cement content (kg/m^3)	340
Fine aggregate (kg/m^3)	826
Coarse aggregate (kg/m^3) (20 mm max. size)	980
Aggregate type	Siliceous
Water (kg/m^3)	187
w/c	0.55
Slump (mm)	150
Specified 28-day strength (MPa)	27.6
Test strength (MPa)	33.7

The test parameters were: fire duration, steel ratio (longitudinal reinforcement) and cover thickness. The eccentricity was a constant in this experiment. Tables 3 and 4 show the details of each column. The temperature changes and appearance of the columns were observed and recorded during fire loading. The longitudinal and lateral displacements were measured during the strength tests, which were performed after the columns were exposed to high temperatures. The details will be described in Section 3.3.

3.2. Fire test

The 1500 mm center-portion of the column was subjected to fire to simulate the column under high temperature exposure (Fig. 6). The columns were put into furnace in a group of four to simulate corner columns as shown in Fig. 7. Only two faces of each column were subjected to the fire. The top and bottom of the specimens were restrained from lateral deformation to simulate diaphram action on the corner column in a building. The inner faces between adjacent columns were insulated to eliminate the heating of the inner face.

Table 2
Location of thermocouples within cross-section

	50 mm cover		70 mm cover	
	X (mm)	Y (mm)	X (mm)	Y (mm)
M1	86.1	70.6	122.8	80.8
M2	155.6	110.3	155.6	110.3
M3	294.5	189.7	294.5	189.7
M4	364	229.4	331.2	219
N1	86.1	229.4	122.8	219
N2	155.6	189.7	155.6	189.7
N3	294.5	110.3	294.5	110.3
N4	364	70.6	331.2	80.2
C	225	225	225	225
S1	50	50	70	70
S2	50	250	70	280
S3	400	250	380	280
S4	400	50	380	70

The axial preloading on each column was 490 kN $(0.1f'_c)$ transmitted from an actuator to the top of the specimens through an universal joint. This axial preloading simulates current engineering practice in Taiwan to assure a ductile behavior for the purpose of earthquake resistance. The axial preloading is relatively low, but this low stress ratio is to assure that the columns would not fail under high temperature for a long fire duration. The ball joint was located in an eccentric location to excert eccentric load. The excertrieity was pre-determinal to simulate the forces in a general building.

The columns were loaded for about 30 min before the start of the fire test and this load was maintained until no further increase in axial deformation. The reason was to mininize the effect of sustained deformation (creep). Then the fire loading was applied. The duration of the fire was predetermined to be 2 or 4 h, which is a time period often used in previous studies [9–11], and the building code in this country specifies a maximum fire resistance of 4 h. The axial preloading was maintained during fire test. Furnace temperatures and pressure variations were monitored in accordence with the standard [37].

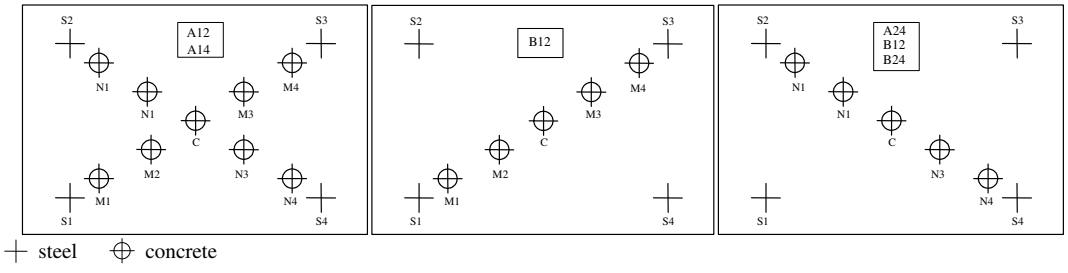

Fig. 9. Location of thermocouples within cross-section (detail size ref. Table 2).

Table 3
Column specimen data

Specimen	Thickness of cover (mm)	Longitudinal reinforced (mm)	Steel ratio (%)	Fire duration (h)
A12	50	No. 8 (φ 25 mm)	1.8	2
A22	50	No. 10 (φ 25 mm)	2.9	2
B12	70	No. 8 (φ 32 mm)	1.9	2
A14	50	No. 8 (φ 25 mm)	1.8	4
A24	50	No. 10 (φ 32 mm)	2.9	4
B24	70	No. 10 (φ 32 mm)	3.0	4

Table 4
Specimen description

First code	Thickness of cover (mm)	Second code	Longitudinal reinforced (mm)	Third code	Fire duration (h)
A	50	1	No. 8 (φ 25 mm)	2	2
B	70	2	No. 10 (φ 32 mm)	4	4

For example A12: cover 50 mm, main bar φ 25 mm, fire duration 2 h.

Finally, the preloadings were removed after the fire test. The furnace cover was lifted 6–12 h after the fire test to cool the specimens. The columns were removed and the exposed surfaces were observed.

3.3. Strength test

The second stage of the experiment was to determine the residual strength of the specimens. An universal joint was employed to evenly distribute the forces from the actuator to the top of the specimens, as shown in Fig. 10. Six linear variable differential transducers (LVDT) were attached to the specimens at mid-height of the column to measure the longitudinal and lateral displacements. Fig. 11 shows the set-up of the LVDT's. The curvatures and strains were calculated from the measurements as shown in Fig. 12. Residual strengths of the columns (P_{ult}) under biaxial loadings after the fire tests were measured. The same eccentricity was used as in the fire-loading test. The strain and curvature along X-axis can be calculated by using Eqs. (9)–(12) as shown in Fig. 12.

$$\varepsilon_{ax} = \frac{\Delta_{ax}}{800}; \quad \varepsilon_{bx} = \frac{\Delta_{bx}}{800} \tag{9}$$

$$d = \left[\frac{\varepsilon_{ax}}{\varepsilon_{ax} + \varepsilon_{bx}}\right] \times 400 \tag{10}$$

$$\varepsilon_{fx} = \frac{\varepsilon_{ax}}{d} \times [d + 25]; \quad \varepsilon_{ux} = \frac{\varepsilon_{bx}}{400 - d} \times [450 - d - 25] \tag{11}$$

$$\varphi_x = \left(\frac{\varepsilon_{fx} + \varepsilon_{ux}}{450}\right) \tag{12}$$

where 800 is the gage length of LVDT at mid-height of column (mm); 400 the spacing between a and b, and c and d (mm); Δ_{ax}, Δ_{bx} the displacements from LVDT along X-axis at a and b (mm); ε_{ax}, ε_{bx} the strains calculated from Δ_{ax}, Δ_{bx} along X-axis at a and b; $\varepsilon_{fx}, \varepsilon_{ux}$ the predicted strains at two edges along X-axis; φ_x is the curvature of X-axis.

The same algorithm was also applied to the Y-axis. The Δ_{cy}, Δ_{dy}, ε_{cy}, ε_{dy}, ε_{fy}, ε_{uy} and φ_y can be obtained in a similar procedure along the Y-axis as shown in Fig. 12. The strain ε_{ux} and ε_{uy} can be calculated from the measured displacements along the respective axis, and the two values (ε_{ux} and ε_{uy}) were found to be close to each other. This verified that the assumptions of plane remain plan in RC theory still holds. Take specimen B24 for example, the deformations from LVDT were 1.047 and 1.973 mm, respectively, along the X-axis, and the calculated ε_{ux} was 0.0025. The deformations from LVDT along the Y-axis were −1.651 and 2.14 mm, respectively, and the calculated ε_{uy} was 0.0021. The difference was almost 16%. The reason for this difference may be due to the local material variation after high temperature where the measuring instruments were mounted.

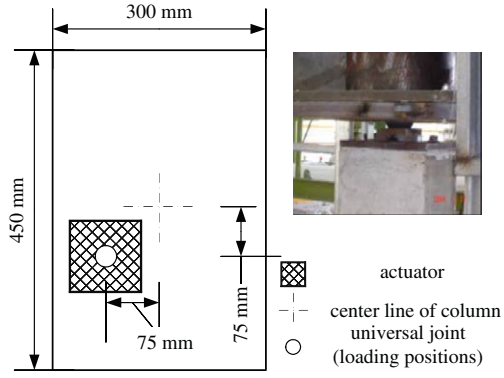

Fig. 10. Column arrangement and load application during strength test.

4. Numerical model

The numerical method is a good and convenient approach to simulate the test result described in the introduction. Assumptions used in the RC analysis are found in many textbooks and are adopted in the present paper, such as the plan remains plan and the tensile strength of concrete is neglected. The concept of the numerical method concept is shown in Fig. 13.

The nominal axial strength was calculated according to the following procedures (Fig. 14 shows the flowchart):

(1) Mesh the column section into $M \times N$ elements.
(2) Identify the temperatures at the four corners of each element by interpolating the thermal couple readings.
(3) Calculate the average temperature (T_{av}) from step (2).
(4) Calculate the residual strength (f_r) of each element from Eqs. (2) or (3) and the maximum strain (ε_{max}) from Eq. (4). Use T_{av} from step (3) as T in Eqs. (2)–(4).
(5) For a given column, assume an initial strain ($\varepsilon_0 = 0.001$) of extreme fiber and a neutral axial with distance c from the surface. The strain at the center of

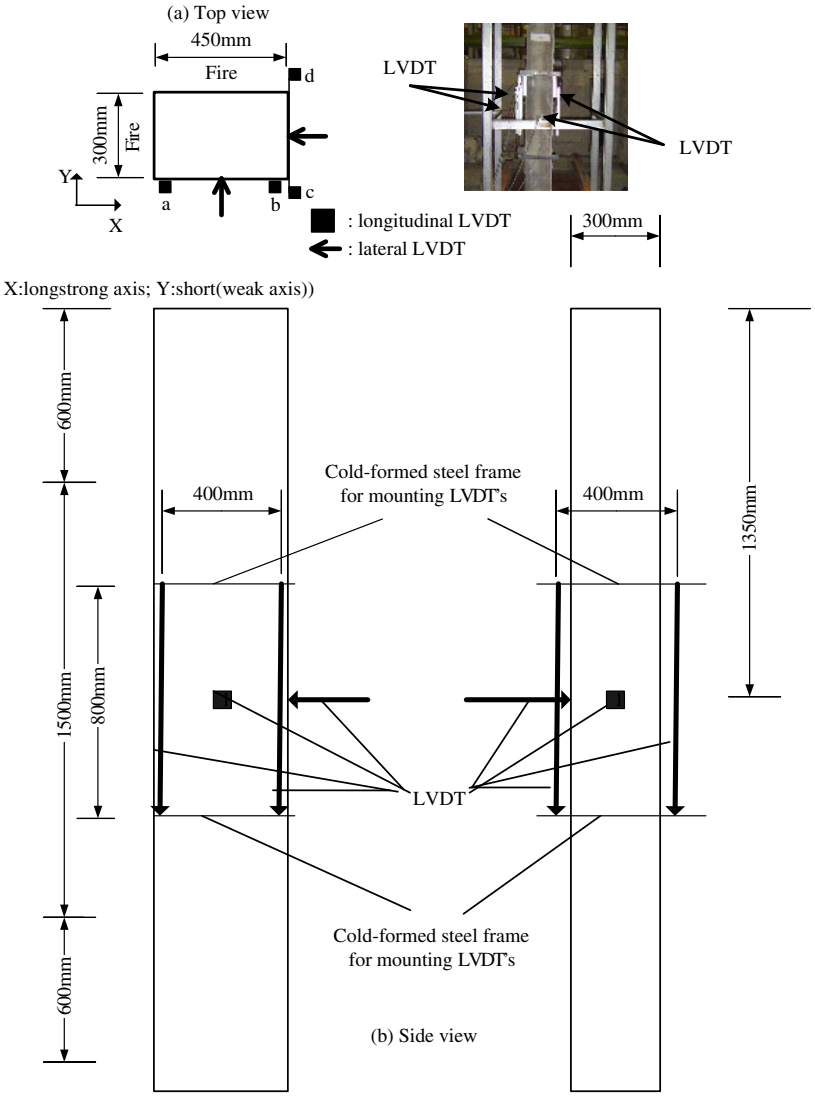

Fig. 11. Lvdt's setup during strength test.

steel and concrete elements could be found with the assumption that the plan remains plan.

(6) For each element, using the strain from step (5), calculate the stress of concrete f_c from Eq. (5) or from Eq. (6) based on f_r from step (4), and steel f_s from Eq. (7) or from Eq. (8). The forces of steel and concrete elements are determined as the product of the element stress multiplied by the element area.

(7) Sum all elements forces and check whether the column resultants of the internal axial forces are in equilibrium with the external forces. If not, then go back to step (5) and assume another neutral axial distance c.

(8) The axial force P_n and moment M_n corresponding to the selected neutral axial distance c and ε_0 can be determined ($M_n = P_n \times$ eccentricity).

(9) Increase a small strain ($\Delta\varepsilon$) on ε_0, and repeat steps (5)–(8). The column axial strength is the maximum value of this procedure.

The axial strength of a column under biaxial loading is calculated by the Bresler reciprocal method [42,43]. The equations are

$$P_0 = 0.85 \times f'_c \times (A_g - A_{st}) + f_y \times A_{st} \tag{13}$$

$$\frac{1}{P_n} = \frac{1}{P_{nx0}} + \frac{1}{P_{ny0}} - \frac{1}{P_0} \tag{14}$$

where P_n is the approximate value of nominal load in biaxial with eccentricities e_x and e_y (kN); P_{ny0} the nominal load when only eccentricity e_x is present ($e_y = 0$) (kN); P_{nx0} the nominal load when only eccentricity e_y is present ($e_x = 0$) (kN); and P_0 is the nominal load for concentrically loaded column (kN).

The effect of temperature gradient depends on the mesh size. To determine the optimal mesh size, a sensitivity analysis was performed. Square elements were used with a mesh of a size of 5, 10, 30, 50, and 150 mm, respectively. As an

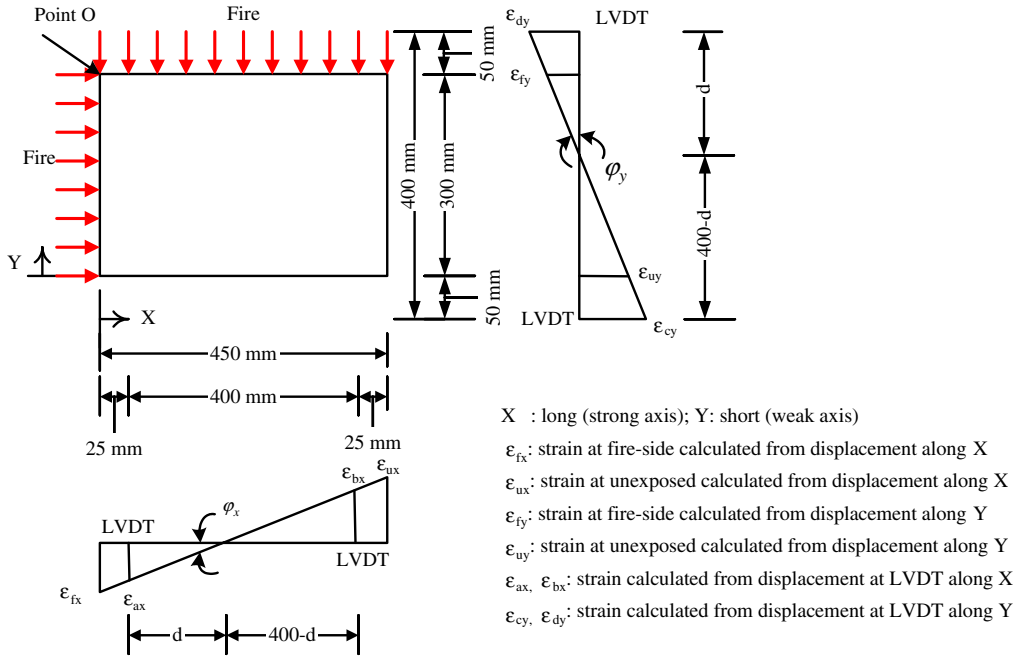

Fig. 12. A sketch map of numerical method.

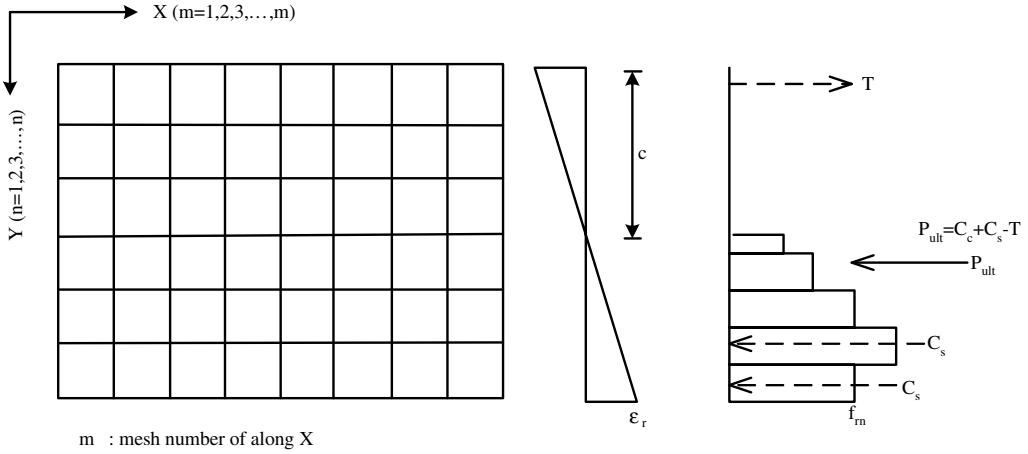

Fig. 13. A sketch map of numerical method.

illustration, the results from specimen A24, are shown in Fig. 15. It is found that the 50 mm element size yields good results. The difference of the calculated axial load strengths between the 50 mm element and the 10 mm element is about 2%. For the sake of convenience, the 50 mm element size is used in this numerical study and gives a conservative results.

5. Experiment results and discussion

5.1. Temperature vs. time

For illustration, Table 5 shows the temperatures at different locations and at different times for specimen A24. The origin of Table 5 was at the junction of two faces

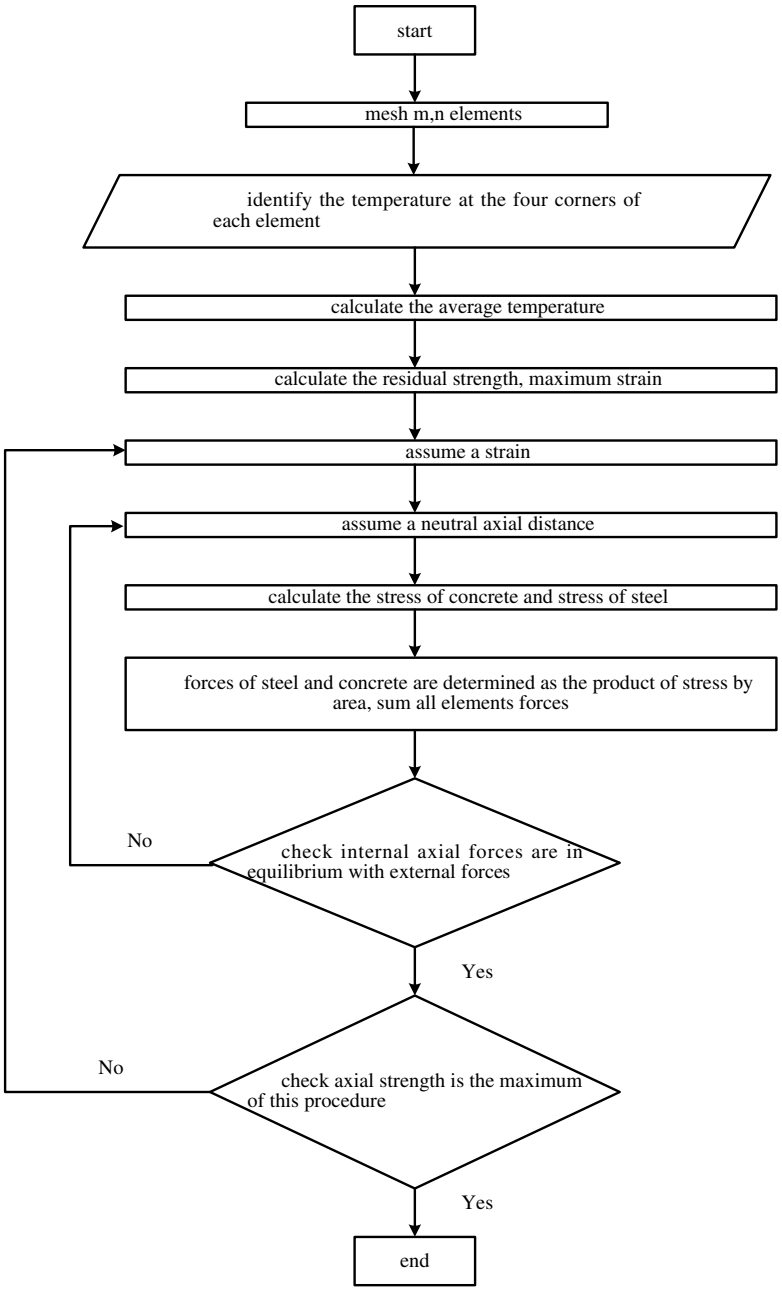

Fig. 14. Flowchart of the analysis procedures.

exposed to the fire (point o in Fig. 12). Test results were as follows: (a) after 4 h of fire, the temperatures at the depth of the concrete cover (coordinate (50 mm, 150 mm)) and at 1/3 the depth of the long axis from fire the surface (coordinate (150 mm, 150 mm)) were 700 and 250 °C, respectively, as shown in Fig. 16, (b) after 2 h of fire, the temperatures at the depth of the concrete cover (coordinate (50 mm, 150 mm)) and at 1/3 depth of the long axis from the fire surface (coordinate (150 mm, 150 mm)) were 600 and 100 °C, respectively, as shown in Fig. 16, and (c) the temperature of the interior concrete continued to increase after the fire test was stopped. For example, the temperature at the center point of the cross-section was still increasing at 2–3 h after the fire test ended, while the temperature at the location of (coordinate (86.1 mm, 70.6 mm)) stopped rising 1 h after the fire test. This is due to the fact the concrete at exterior with higher temperature, transfers heat into the inner concrete with lower temperature, thus raises the temperature of inner concrete.

Table 6 shows that the temperatures at the center points of all specimens. It is found that: (a) the heat transfer was not affected by the cover thickness or the steel ratio, and (b) the average temperature at the center was 151.9 and

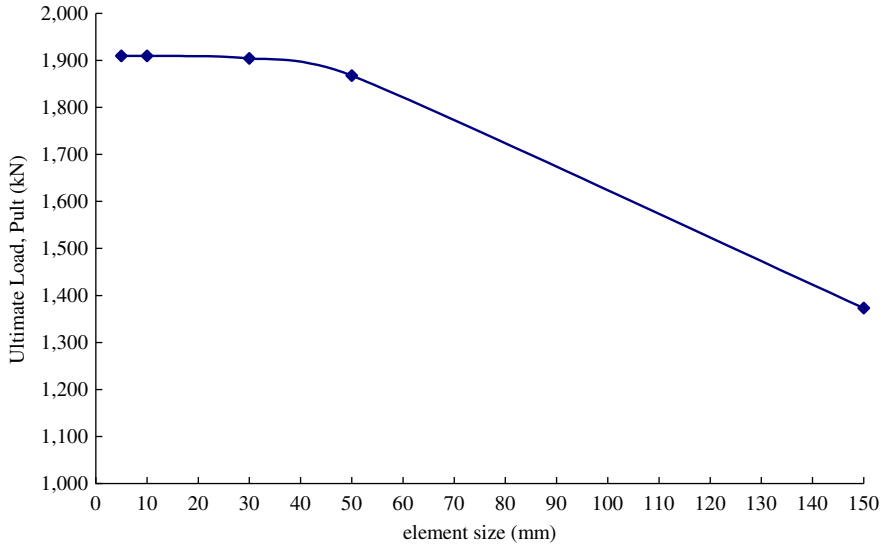

Fig. 15. Mesh size vs. P_{ult} effect.

Table 5
Cross-section temperature and time data (°C) (A24)

X (mm)	86.1	155.6	225	294.5	364	50	50	400	400
Y (mm)	70.6	110.3	150	189.7	229.4	250	50	50	250
0 h	27.4	27.3	26.8	27.3	27.2	26.9	27.6	27.0	26.7
1 h	102.7	88.0	66.6	42.6	39.9	108.1	168.9	150.7	36.7
2 h	209.2	128.9	109.4	82.9	72.6	200.3	365.5	255.8	64.1
3 h	338.5	216.6	124.3	106.3	104.0	292.8	523.9	336.9	96.3
4 h	452.2	308.7	173.4	117.1	111.2	378.2	644.9	407.8	106.3
5 h	508.3	377.1	221.5	145.1	130.2	409.9	593.8	389.5	125.0
6 h	464.3	389.3	257.2	177.8	159.0	367.9	479.0	321.4	147.5
7 h	409.9	367.6	268.6	196.1	175.3	326.6	400.4	275.8	160.9

101.9 °C after the 4 and 2 h tests, respectively. This was only about 50 °C difference.

An isothermal contour for the column cross-section was plotted based on the experimental data at various times. Fig. 16 shows that heat was transferred into the concrete column mainly from their two heated sides for each column as expected. However, a small amount of heat was transferred from the interface between the concrete faces due to column deformation during the test. However, this effect was not significant, and the heated outer 1/3 portion of the columns from fire the surface showed an increase of temperature about of 100 °C in the shaded area (Fig. 16). This area is only 3.4% of the total area and the reduction of concrete material strength in this area is only 10% from Eq. (2). Therefore, the effect of this small amount of heat from the interface is not important. Meanwhile, in real situations, the fire will reach the rear faces of an exterior column due to the aerodynamic characteristics of fire, which was close to the test condition.

The temperature distribution of the concrete, within the cross-section can be done through direct measurement. The temperatures can also be calculated by a finite difference method. The heat balance equation was as per Eq. (15)

$$\frac{\partial T}{\partial t} = \frac{k}{c\rho}\left(\frac{\partial^2 T}{\partial x^2} + \frac{\partial^2 T}{\partial y^2}\right) \tag{15}$$

where T is the temperature (°C); t the time (min); k the thermal conductivity ($W\,m^{-1}\,°C^{-1}$); ρ the density ($kg\,m^{-3}$); and c is the specific ($J\,kg^{-1}\,°C^{-1}$).

The cross-section of the column is idealized as a network of elements by solving the heat balance equation. Detailed descriptions are provided in Refs. [15–17] and are not given here. This study solved the heat balance equation and compared the calculated results with the experimental data, as shown in Table 7. It shows that the numerical method is a good approach and is justified. This study used experimental data for strength analysis. However, the numerical approach can be further used for different dimensions or for RC structural elements without prior experimental results.

Under the axial compressive stress ratio ($0.1f'_c$), the temperature distribution across the section is not affected by the concrete cover thickness or steel ratio. The effect of the axial stress ratio on the temperature distribution across the section is not a subject in this research. This effect is not considered in most literatures either [9,10,13–17].

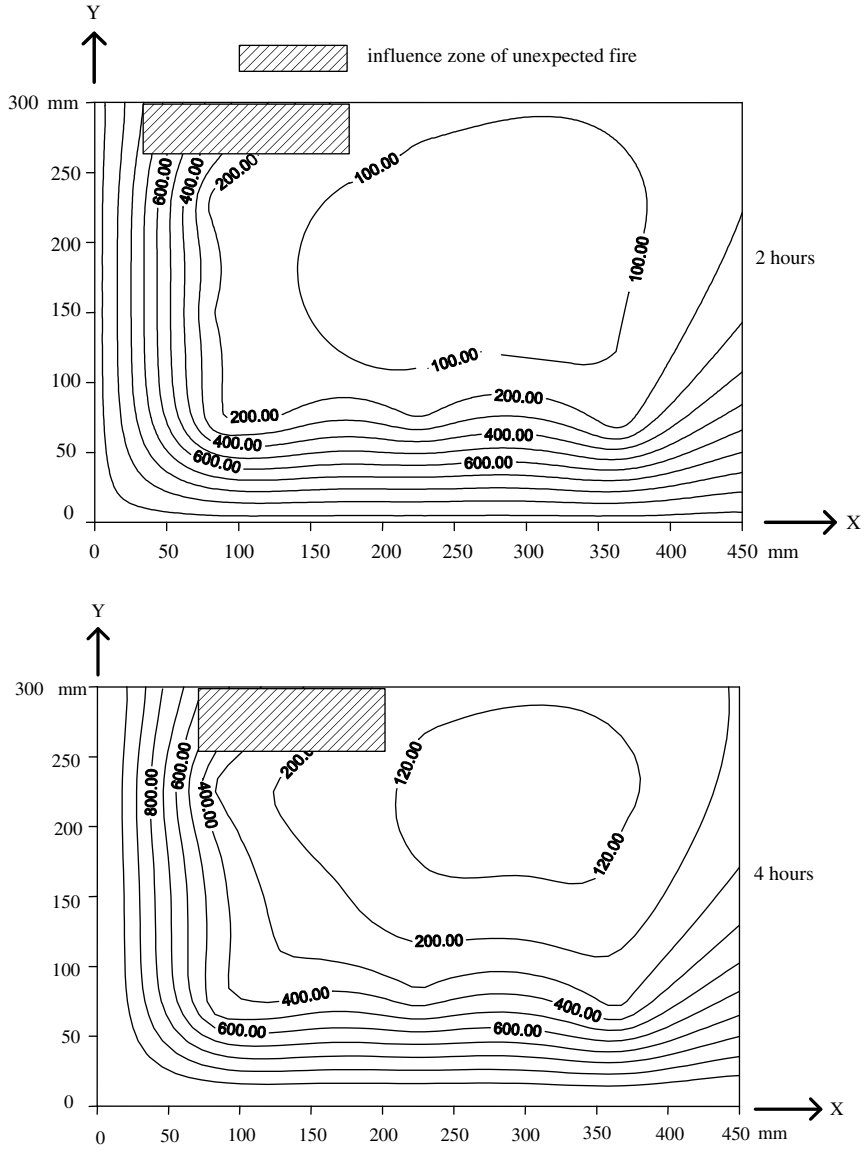

Fig. 16. Temperature contour at 2 and 4 h.

Table 6
Temperature of center point vs. time (°C)

Specimen	1 h	2 h	3 h	4 h
A12	66.0	107.8		
A22	50.8	103.8		
B12	53.9	95.1		
A14	51.5	95.1	113.5	132.7
A24	66.6	109.4	124.3	173.4
B24	–	100.0	108.5	149.6
Average temperature	57.8	101.9	115.4	151.9

5.2. Surface observation after fire tests

Each specimen was carefully observed after removal from the furnace (Fig. 17). It was found that: (a) the color was in general yellowish, and the longer the fire duration, the darker the color, (b) numerous fine-networked cracks were observed, (c) at the end of fire test, longitudinal cracks were found at the depth of the concrete cover over about 300–750 mm of the length of the exposed region. Please note that the length of the exposed region is 1500 mm. A lager longitudinal cracks occurred on the surface of column B24 (cover 70 mm and 4 h fire duration) but all within the depth of concrete cover. The others columns also showed longitudinal cracks, but crack widths were relative smaller than those of B24, and (d) only very few "spot" spalls of 2 mm in depth were observed on the exposed surfaces; the area of the spall is 3% of the expose area and the spots were not connected to longitudinal cracks (also see Fig. 17). The study in Section 3.1 wants to stress the longitudinal cracks but not the spalls. In fact, longitudinal cracks at the depth of cover

Table 7
Temperature from test and prediction (°C)

Coordinate (X, Y)	(86.01 mm, 70.6 mm)		(155.6 mm, 110.3 mm)		(225 mm, 150 mm)		(294.5 mm, 189.7 mm)		(364 mm, 229.4 mm)	
	Test	Predict	Test	Predict	Test	Predict	Test	Predict	Test	Predict
1 h	106.2	239.73	94.5	79.82	57.8	36.84	45.2	24.22	41.1	21.21
2 h	215.2	447.75	128.9	200.43	101.9	97.78	88.7	51.12	80.3	32.42
3 h	318.0	586.53	204.9	307.47	115.4	165.16	101.2	90.178	96.5	54.86
4 h	425.4	692.83	294.3	396.07	151.9	229.58	106.6	131.33	101.6	82.19

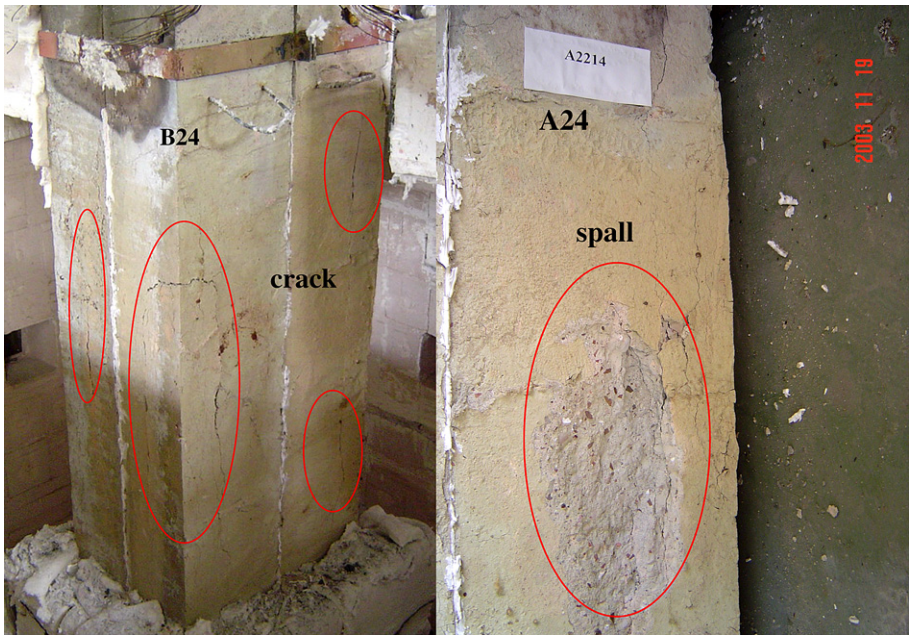

Fig. 17. Crack and spalls of specimens after fire test.

were observed together with very minor "spot" spalls, as expected.

Further investigation of the test results demonstrated that the parameters affecting the initiation of cracks or spall-offs in sequence of the importance were fire duration, cover thickness, and size of steel. The tests also showed that: (a) the less the steel ratio, the less the cracks, (b) the smaller the cover thickness, the less the cracks, and (c) the shorter the fire duration, the less the cracks.

5.3. Lateral displacements, and curvature

The curvatures were calculated from the measurement of lateral and longitudinal displacements during the strength tests. It was found that longer fire duration resulted in a smaller radius of curvature (Fig. 18). As to the measured lateral displacements, it was found that the specimens showed a lateral displacements in the range of 7–25 mm, mainly from material asymmetry across the cross-section after uneven fire loading and eccentric axial loading (Fig. 19).

It can be found that: (1) for the same design conditions, the longer fire duration and the higher temperature result in lower modulus of elasticity (E) and flexural stiffness (EI), and the curvature and displacement are higher based on the mechanics of the materials; (2) for the same fire duration, a larger cover, which means a smaller core area, yields a lower moment of inertia (I) and flexural stiffness (EI), and the curvature and displacement are higher based on the mechanics of the materials, because in general a longitudinal cracks occur at the depth of cover.

5.4. Residual strength

Table 8 shows the calculated strength of the specimens at room temperature. The calculated results were compared with the ACI 318 code and the difference is about 5%. Table 9 shows the calculated residual strength of the specimens after fire as per the procedures described in Section 4. The calculated results were compared with the experimental results and were found conservative. Table 10 lists the residual strength ratios of the specimens. The following relationships for residual strength ratios were found:

(a) The longer the fire, the less the residual strength ratio (Table 10-(1)). Duration contributes a 10% reduction

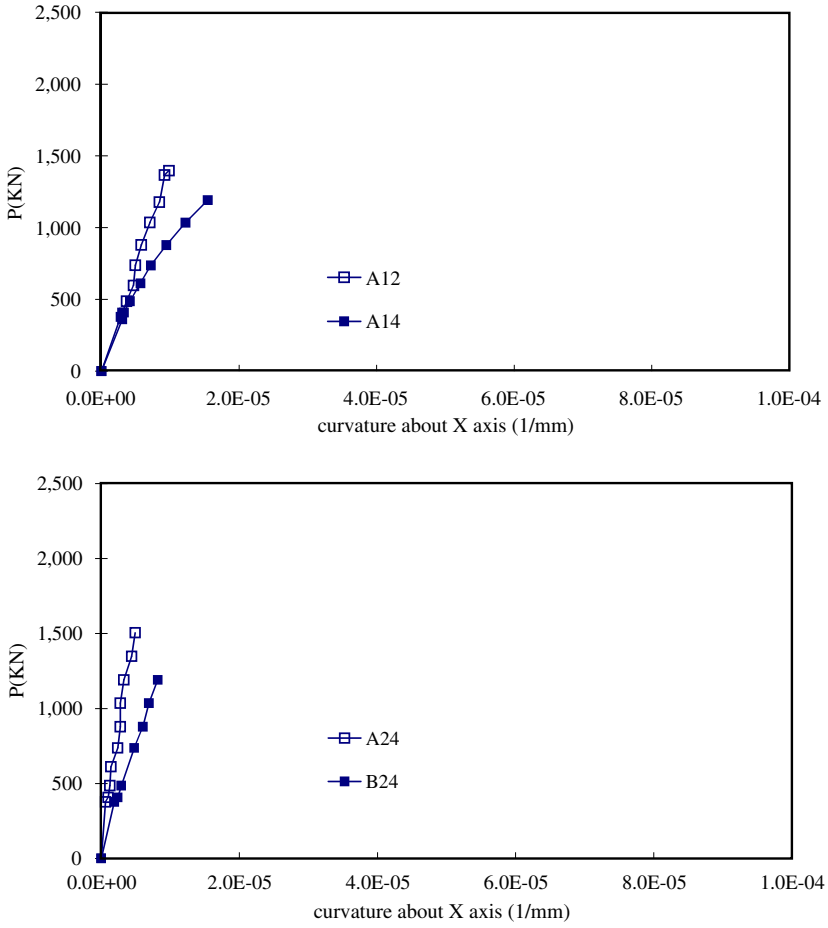

Fig. 18. P–ϕ about X-axis.

on residual strength as it changes from 2 to 4 h. The reason for the small difference may be due to the fact that the temperature distribution across the column sections under different fire durations is not significantly different and the temperature is not high enough at the center of the concrete cross-section to cause a substantial strength reduction.

(b) Table 10-(2) shows that the ratios were 65.24% and 57.29% for the 4-h tests with 3% and 2% steel ratio. The ratio was 67.09% for the 2-h tests with 2% steel ratio. From the analytical results it is shown that the less the steel ratio, the less the residual strength ratio.

(c) The residual strength ratios were 56.44% and 67.09% for the 2-h tests with concrete cover of 70 and 50 mm (Table 10-(3)). The residual strength ratios were 55.66% and 65.24% for 4-h tests with concrete covers of 70 and 50 mm (Table 10-(3)), respectively. That is, the thicker the cover, the less the residual strength ratio. In other words, the less the cover, the larger the core area, thus the larger the residual strength ratio. Only the core area, which is subjected to the confinement of ties, contributes to the axial strength for columns.

(d) This study was compared with Lin [10] to find the difference in the behavior of eccentrically loaded interior columns and corner columns. Table 11 shows the difference in design of the two tests. Although the variables are not the same, the trend on residual strength can be a reference to engineers. It was found that: (a) columns from both tests show a similar appearance in color, (b) at the same fire duration, the corner column has a higher residual strength ratio than the interior column. Also shown in Table 12, the residual strength ratios ranged between of 60.56–63.29% for 2 h fire duration of this study, while residual strength ratios were in the range of 59.3–50.2% for 2 h from the Lin's study. The reason for this is that the interior columns were exposed on four-sides, which caused higher temperatures in columns, and (c) as the duration changes from 2 to 4 h, the decrease of the residual strength ratio for the corner column is less than that for the interior column, for the same reasons selected in (b). Also shown in Table 12, a decrease of the analysis residual strength ratio of about 10% for the corner columns and a decrease of the residual strength ratios about 10–15% for the interior columns.

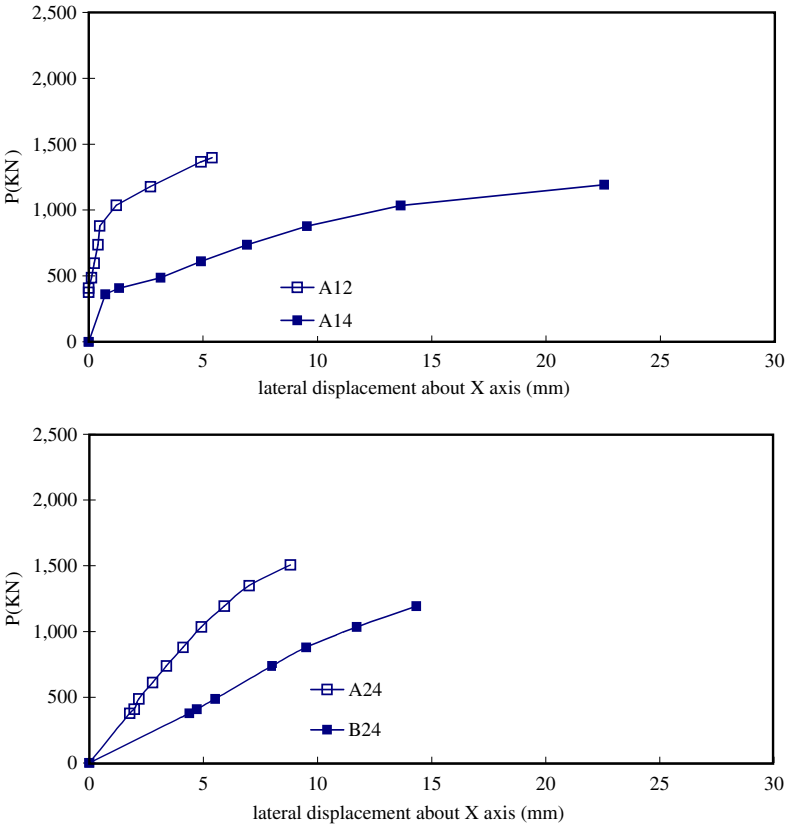

Fig. 19. P–Δ about X-axis.

Table 8
Predicted strength for room temp

	ACI, kN	Research, kN
A10	1979.49	2080.25
A20	2183.14	2307.21
B10	1833.72	1930.00

Table 9
Residual strength (P_{ult})

Specimen	Test, kN	Analysis, kN	Test/analysis
A12	1395.52	1259.84	1.11
A22	[a]	1460.14	–
B12	1034.88	1136.51	0.91
A14	1191.68	1107.57	1.08
A24	1505.28	1310.70	1.15
B24	1191.68	1184.63	1.01

The principal variables were underlined.
[a] Test error.

6. Conclusion

Based on the data presented and discussed herein, the following conclusions can be drawn:

– The dimensions of the core of the column are very important for the residual strength. For the same fire duration, the larger core area gives a higher residual strength. The thicker the cover, the earlier the cover tends to fall off. The column strength depends mainly on the core of concrete. Therefore, if the core area is increased, the RC column will have a higher residual strength after high temperature exposure. This statement also holds for columns not affected by high temperature.
– The factors affecting initiation of cracks are, in sequence of importance, fire duration, concrete cover thickness, and steel ratio. However, the existence and the characteristics of surface cracking after fire are not directly related to strength loss.
– The temperature in the interior part of the specimen continued to rise even after the furnace was turned off. That is, the temperature of the exterior part of the specimen was decreasing while the temperature of the interior was increasing. This difference may cause secondary damage to the column and further complicates analysis.
– The investigation of the residual strength ratios shows that: (a) the longer the fire, the less the residual strength ratio, (b) the less the steel ratio, the less the residual strength ratio, and (c) the thicker the cover, the less the residual strength ratio.
– Fire safety behavior of concrete was and is an important topic in building. This study only focused on low-rise buildings, which have a lower axial load. High-rise building is a different issue. It involves high strength

Table 10
Residual strength (Pult) ratios

(1) Fire duration (2 h. vs. 4 h.)			(2) Steel ratio (2% vs. 3%)			(3) Cover (50 mm vs. 70 mm)		
Specimen	Test (%)	Analysis (%)	Specimen	Test (%)	Analysis (%)	Specimen	Test (%)	Analysis (%)
A12	67.09	60.56	A12	67.09	60.56	A12	67.09	60.56
A14	57.29	53.24	A22	–	63.29	B12	56.44	58.89
A22	–	63.29	A14	57.29	53.24	A24	65.24	56.81
A24	65.24	56.81	A24	65.24	56.81	B24	55.66	55.33

The principal variables were underlined.

Table 11
Column specimen data for four-sides and two sides test

	This study (A1X)	This study (A2X)	Lin (1)	Lin (2)
f'_c(MPa)	33.7	33.7	19.40	20.48
f_y (MPa)	475.87	475.87	354.76	354.76
Aggregare	Siliceous	Siliceous	Siliceous	Siliceous
Cross-section	300 × 450 mm	300 × 450 mm	400 × 400 mm	300 × 300 mm
Cover (mm)	50 mm	50 mm	50 mm	50 mm
Main bar (mm)	No. 8 (φ 25 mm) × 4	No. 10 (φ 32 mm) × 4	No. 7(φ 22 mm) × 6	No. 7 (φ 22 mm) × 4
Steel ratio	0.018	0.029	0.015	0.017
Stirrup (mm)	No. 4 (φ 13 mm)	No. 4 (φ 13 mm)	No. 3 (φ 10 mm)	No. 3 (φ 10 mm)
Fire duration (h)	2, 4	2, 4	2, 4	2, 4
Eccentricity	$e_x = e_y = 75$ mm	$e_x = e_y = 75$ mm	$e_x = 200$ mm	$e_x = 150$ mm
Fire curve	CNS 12515	CNS 12515	BS 476	BS 476
Fire sides	2	2	4	4

Table 12
Residual strength ratios of eccentrically loaded interior column and corner column

Duration (h)	This study (A1X)		This study (A2X)		Lin (1)		Lin (2)	
	Test (%)	Analysis (%)	Test (%)	Analysis (%)	Test (%)	Analysis (%)	Test (%)	Analysis (%)
2	67.09	60.56	–	63.29	53.9	59.3	56.2	50.2
4	57.29	53.24	65.24	56.81	39.4	49.4	29.15	35.9

material, slender columns, and high axial forces. Their behavior is more complex and they were not included in this study. The findings of this study of residual strengths can be used for future evaluation, repairs and strengthening.

Acknowledgement

The authors would like to thank the Architecture and Building Research Institute (ABRI), Ministry of the Interior, ROC for funding of this research under contract No. 092-301070000-G1020.

References

[1] Lie TT, Rowe TT, Lin TD. Residual strength of fire-exposed reinforced concrete column. ACI Publication SP 92; 1984. p. 153–74.
[2] Lie TT, Lin TD. Fire performance of reinforced concrete columns. ASTM Special Technical Publication 1985. p. 176–205.
[3] Lie TT, Lin TD. Influence of restraint on fire performance of reinforced concrete columns. Proceedings of the first international symposium on fire safety science; 1986. p. 291–300.
[4] Lie TT, Celikkol B. Method to calculate the fire resistance of circular reinforced concrete columns. ACI Mater J 1991;88(1):84–91.
[5] Lin TD, Zwiers RI, Burg RG, Lie TT, McGrath RJ. Fire resistance of reinforced concrete columns. Research and development bulletin RD101B. Skokie (IL): Portland Cement Association; 1992.
[6] Ng AB, Mirza MS, Lie TT. Fire endurance analysis of reinforced concrete columns. Can J Civil Eng 1989;16(3):290–9.
[7] Ng AB, Mirza MS, Lie TT. Response of direct models of reinforced concrete columns subjected to fire. ACI Struct J 1990;87(3):313–25.
[8] Purkiss JA, Weeks NJ. Computer study of reinforced concrete columns in fire. Struct Eng Part B 1987;65B(1):22–8.
[9] Lin CH, Chen ST, Hwang TL. Residual strength of reinforced concrete columns exposed to fire. J Chinese Inst Eng 1989;12(5): 557–65.
[10] Lin CH, Tsay CS. Deterioration of strength and stiffness of reinforced concrete columns after fire. J Chinese Inst Eng 1990;13(3):273–83.
[11] Lin CH, Chen ST, Yang CA. Repair of fire-damaged reinforced concrete columns. ACI Struct J 1995;92(4):406–11.
[12] Terro MJ. Numerical modeling of the behavior of concrete structures in fire. ACI Struct J 1998;95(2):183–93.
[13] Kodur VKR, Sultan MA. Structural behavior of high strength concrete columns exposed to fire. In: International symposium on high performance and reactive powder Concrete, Sherbrooke, Quebec; 1998. p. 217–32.
[14] Kodur VKR, McGrath R. Fire endurance of high strength concrete columns. Fire Technol 2003;39:73–87.
[15] Kodur VKR, Cheng FP, Wang TC. Effect of strength and fiber reinforcement on fire resistance of high-strength concrete columns. J Struct Eng – ASCE 2003;129(2):253–9.

[16] Kodur VKR, Cheng FP, Wang TC. Predicting the fire resistance behavior of high strength concrete columns. Cement Concrete Comp 2004;26(2):141–53.
[17] Kodur VKR. Guidelines for fire resistance design of high-strength concrete columns. J Fire Protect Eng 2005;15(2):93–106.
[18] Kodur VKR, Bisby LA, Green MF, Chowdhury E. Fire endurance of insulated FRP-strengthened square concrete columns. In: Proceedings of the 7th international symposium on fiber-reinforced (FRP) polymer reinforcement for concrete structures, SP-230-71; 2005. p. 1253–68.
[19] Kodur VKR, Bisby LA, Green MF. Experimental evaluation of the fire behavior of insulated fiber-reinforced-polymer-strengthened reinforced concrete columns. Fire Safety J 2006;41(7):547–57.
[20] Dotreppe JC, Franssen JM, Vanderzeypen Y. Calculation method for design of reinforced concrete columns under fire conditions. ACI Struct J 1999;96(1):9–18.
[21] Franssen JM, Dotreppe JC. Fire tests and calculation methods for circular concrete columns. Fire Technol 2003;39:89–97.
[22] Zha XX, Li LY, Purkiss JA. Finite element analysis of the fire resistance of reinforced concrete columns. In: Proceedings of the eight international conference on civil and structural engineering computing; 2001. p. 161–2.
[23] Tan KH, Yao Y. Fire resistance of four-face heated reinforced concrete columns. J Struct Eng – ASCE 2003;129(9):1220–9.
[24] Tan KH, Tang CY. Interaction formula for reinforced concrete columns in fire conditions. ACI Struct J 2004;101(1):19–28.
[25] Tan KH, Yao Y. Fire resistance of reinforced concrete columns subjected to 1-, 2-, and 3-face heating. J Struct Eng – ASCE 2004;130(11):1820–8.
[26] Faris A, Ali N, Gordon S, Abid AT. Outcomes of a major research on fire resistance of concrete columns. Fire Safety 2004;39(6):433–445.
[27] Chung JH. Consolazio GR. Finite element stress analysis of a reinforced high-strength concrete column in severe fires. In: Proceedings of the 2004 structures congress – building on the past: securing the future; 2004. p. 1183–90.
[28] Persson B. Fire resistance of self-compacting concrete, SCC. Mater Struct 2004;37:575–84.
[29] Bratina S, Cas B, Saje M. Numerical modeling of behavior of reinforced concrete columns in fire and comparison with Euro code 2. Int J Solids Struct 2005;42(21–22):5715–33.
[30] Benmarce A, Guenfoud M. Experimental behavior of high-strength concrete columns in fire. Therm Sci 2007;l1(2):37–52.
[31] Benmarce A, Guenfoud M. Behavior of axially restrained high strength concrete columns under fire. Construct Build Mater 2005; 57(5):283–7.
[32] ACI Committee 363. State of the art report on high strength concrete. American Concrete Institute, Detroit; 1997.
[33] Neville AM. Properties of concrete, London; 1996.
[34] The Self-Compacting Concrete European Project Group. The European guidelines for self compacting concrete; 2005.
[35] Yunus AC. Heat transfer: a practical approach. McGraw-Hill; 1998.
[36] Hsu JH (advisor: Lin CS.). Numerical modeling of mechanical properties for reinforced concrete beam exposed to fire. PH.D. thesis, Institute of Mechanical Engineering, Yuan-Ze University, Chungli, Taiwan; 2005.
[37] CNS 12514. Method of fire resistance test for structural parts of building. Chinese National Standard 2005.
[38] ISO 834. Fire resistance tests – elements of building construction. International Organization for Standardization 1999.
[39] Chang CH (advisor: Jau WC.). Study of fired concrete strengthened with confinement. MS thesis, National Chiao Tung University, Hsinchu, Taiwan; 2001.
[40] Schneider U, Haksever A. Bestimmung der aguivalenten brandauer von statisch bestimmt gelagerten stahlbetonbalken bei Naturlichen Branden. Bericht des Technischen Iniversit at Braunschweig; 1976.
[41] Malhotra HL. Design of fire resisting structures. New York: Chapman & Hall; 1982.
[42] ACI Committee 318. Building code requirements for reinforced concrete (ACI 318-02). American Concrete Institute, Detroit; 2002.
[43] Bresler B. Design criteria for reinforced columns with Biaxial bending. ACI J 1960;57(110):481–90.